

# Development of an Amino Sugar-Based Supramolecular Hydrogelator with Reduction Responsiveness

Sayuri L. Higashi and Masato Ikeda\*



Cite This: *JACS Au* 2021, 1, 1639–1646



Read Online

ACCESS |



Metrics & More



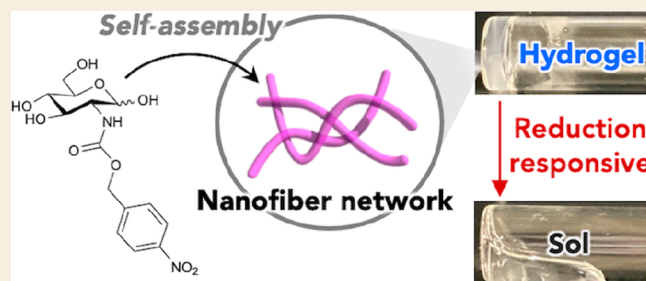
Article Recommendations



Supporting Information

**ABSTRACT:** Stimuli-responsive supramolecular hydrogels are a newly emerging class of aqueous soft materials with a wide variety of bioapplications. Here we report a reduction-responsive supramolecular hydrogel constructed from a markedly simple low-molecular-weight hydrogelator, which is developed on the basis of modular molecular design containing a hydrophilic amino sugar and a reduction-responsive nitrophenyl group. The hydrogel formation ability differs significantly between glucosamine- and galactosamine-based self-assembling molecules, which are epimers at the C4 position, and only the glucosamine-based derivative can act as a hydrogelator.

**KEYWORDS:** supramolecular hydrogel, low-molecular-weight hydrogelator, reduction responsiveness, amino sugar, nitrophenyl group



## INTRODUCTION

Supramolecular hydrogels,<sup>1</sup> which consist of a network of supramolecular nanoarchitectures built from supramolecular hydrogelators (or low-molecular-weight hydrogelators), can be used in a variety of bioapplications, such as drug releasing matrices,<sup>2</sup> sensing materials,<sup>3</sup> and cell-culturing or cell-killing materials.<sup>4</sup> Because supramolecular hydrogels are readily constructed from chemically well-defined supramolecular hydrogelators, various functions can be installed into them, including responsiveness toward specific stimuli, such as pH,<sup>5</sup> light,<sup>6</sup> and redox,<sup>7</sup> via a semirational molecular design and focused trial-and-error screening of hydrogel formation ability.

In this context, the development of reduction-responsive supramolecular hydrogels through semirational molecular design has recently attracted attention<sup>7</sup> because the reduction stimuli can be biocompatible and the dysregulation of reductive conditions in living organisms is known to be associated with certain diseases such as cancer.<sup>8</sup> Specifically, the introduction of a disulfide linkage is considered the most reliable molecular design<sup>7a–c</sup> because this linkage can be readily cleaved under reductive conditions generated upon the addition of reducing agents, such as phosphine derivatives, or in the presence of biorelevant and biocompatible thiols, such as reduced glutathione. In fact, dibenzoyl cysteine, a long-known supramolecular hydrogelator containing a disulfide linkage,<sup>7a</sup> exhibits reduction-responsive gel-to-sol transition.<sup>7c</sup> Other reduction-sensitive chemical groups, such as azo,<sup>7d</sup> ferrocenyl,<sup>7e</sup> phenylselenyl,<sup>7f</sup> and nitro groups,<sup>7g–i</sup> have also been effectively utilized to develop reduction-responsive supramolecular hydrogels.

For the design of self-assembling molecules including supramolecular hydrogelators, carbohydrates are attractive not only because of the presence of multiple hydrophilic hydroxyl groups to modulate the amphiphilic tendency but also their inherent chirality, which facilitates the asymmetric arrangement of the self-assembling molecules to form fibrous supramolecular nanoarchitectures suitable for hydrogel formation.<sup>9,10</sup> In particular, amino sugars including galactosamine (GalNH<sub>2</sub>, 2-amino-2-deoxy-D-galactose) and glucosamine (GlcNH<sub>2</sub>, 2-amino-2-deoxy-D-glucose), which are major components of structural polysaccharides present on the surface of mammalian cells,<sup>11</sup> are useful because they possess a single amino group at the C2 position that serves as an anchor site for the simple and selective conjugation with a variety of functionalities conducive to the self-assembly behavior, including aromatic amino acids and alkyl chains.<sup>12</sup> For instance, Birchall et al. recently reported simple supramolecular hydrogelators derived from amino sugars bearing the fluorenyl-9-methoxycarbonyl (Fmoc) group as a powerful self-assembly facilitating group (referred to as GalN- and GlcN-Fmoc in Figure 1).<sup>13</sup> Following this line, we herein report that the introduction of a 4-nitrophenylmethoxycarbonyl (NPmoc) group, instead of Fmoc, into one of such amino sugars gives rise to a supramolecular hydrogelator (GlcN-NPmoc, Figure

Received: June 15, 2021

Published: July 22, 2021



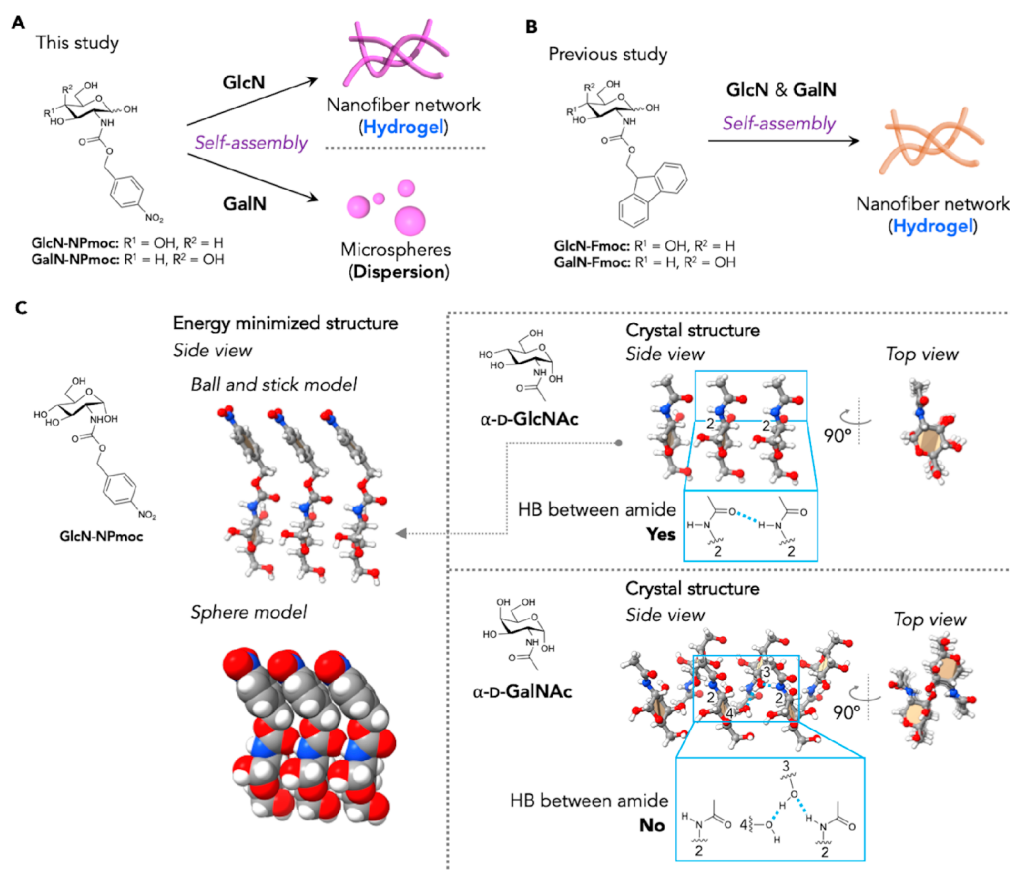


**Figure 1.** (A) Chemical structures and schematic representation of the self-assembly of GlcN- and GalN-NPmoc into a nanofiber network and microspheres, respectively, investigated in this study. (B) Chemical structures of GlcN- and GalN-Fmoc reported previously by Birchall et al.<sup>13a</sup> (C) Energy-minimized self-assembled structure of GlcN-NPmoc (MMFFs) derived from a single-crystal structure of *N*-acetyl- $\alpha$ -D-glucosamine ( $\alpha$ -D-GlcNAc, ACGLUA10)<sup>18a</sup> is shown on the left. The possibility of antiparallel and interdigitated self-assembled structures is not presented but should not be excluded.<sup>13a</sup> The schematic representation for crystal structures of  $\alpha$ -D-GlcNAc and *N*-acetyl- $\alpha$ -D-galactosamine ( $\alpha$ -D-GalNAc, AGALAM10)<sup>18b</sup> is shown on the right.

1), which is more compact than its Fmoc counterpart and, unlike the latter, exhibits the desired reduction-responsive function. The newly developed GlcN-NPmoc, which is a purely organic compound without any transition metal, is one of the simplest low-molecular-weight supramolecular hydrogelators capable of producing reduction-responsive functional supramolecular hydrogels reported to date (Figure S1).<sup>14</sup>

## RESULTS AND DISCUSSION

A straightforward synthesis of NPmoc-carbohydrates, GlcN- and GalN-NPmoc, was carried out according to a previously reported method (Scheme S1).<sup>13a,15</sup> To evaluate the aqueous self-assembling ability of GlcN- and GalN-NPmoc, their stock solutions in dimethyl sulfoxide (DMSO), a water-miscible organic solvent, were mixed with an aqueous buffer, i.e., 100 mM 4-(2-hydroxyethyl)-1-piperazineethanesulfonic acid (HEPES)-NaOH (pH 7.4). The resultant suspensions were heated to obtain clear solutions and then cooled to room temperature to induce the self-assembly. We found that GlcN-NPmoc formed a stable hydrogel above a concentration of approximately 0.75 wt % (21 mM), whereas GalN-NPmoc only produced suspensions (no gel formation was observed even at higher concentrations, e.g., 1.0 wt %), as shown in Figure 2A. We found that the heating-and-cooling process was necessary to obtain the hydrogels (Figure S6). Also, the powders of GlcN-NPmoc were directly mixed with aqueous

media [e.g., HEPES-NaOH (pH 7.4) or MES-NaOH (pH 5.5)], phosphate buffered saline, milli-Q water, or deuterium oxide (D<sub>2</sub>O). Similar heating/cooling treatment of the suspensions gave stable hydrogels and the hydrogel prepared with D<sub>2</sub>O was used for Fourier transform infrared (FTIR) and nuclear magnetic resonance (NMR) spectroscopy study (vide infra). The viscoelastic property of the representative GlcN-NPmoc hydrogels was evaluated through conventional oscillatory rheology experiments (Figure 2B), which indicated the formation of physical hydrogels.<sup>16</sup> As shown in Figure 2B,  $G'$  was higher than  $G''$  and almost no frequency dependence of  $G'$  was observed at lower frequency. The  $\tan \delta$  ( $G''/G'$ ) values (0.14 and 0.12 for [GlcN-NPmoc] = 0.75 and 1.0 wt %, respectively, from frequency sweep at 1.0 rad s<sup>-1</sup>) are within a typical range for this type of low-molecular-weight supramolecular hydrogels.<sup>17</sup> The GlcN-NPmoc hydrogels were stable for several weeks whereas they showed no thixotropy, i.e., no recovery of the original gel state after mechanical breakdown. Nonetheless, the formation of the GlcN-NPmoc hydrogels was thermally reversible and the gel-to-sol transition temperature ( $T_{\text{gel}}$ ) was determined to be 51 °C for a hydrogel concentration of 1.0 wt % in 100 mM HEPES-NaOH (pH 7.4) with DMSO (5.0 vol %). Note that the difference in the hydrogel formation ability between glucosamine-based GlcN-NPmoc and galactosamine-based GalN-NPmoc, which are epimers at the C4 position of the amino sugar, contrasts with

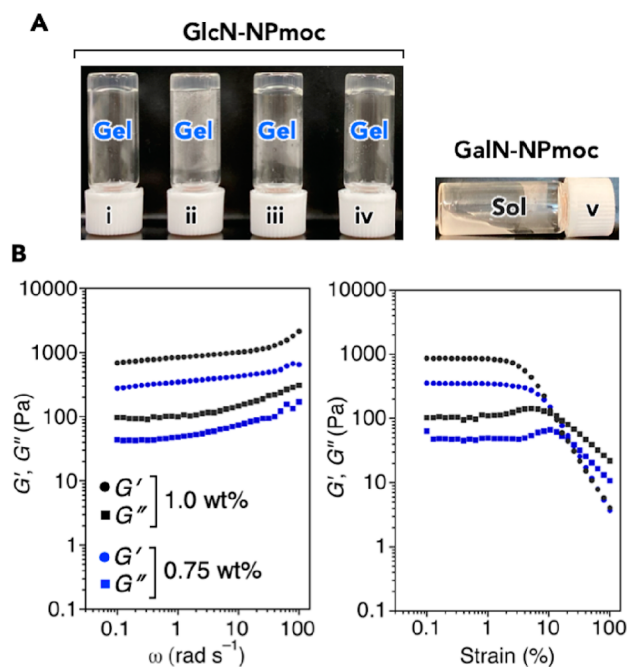


**Figure 2.** (A) Photographs of GlcN-NPmoc hydrogels prepared using 100 mM HEPES–NaOH (pH 7.4) (i) with or (ii) without DMSO (5.0 vol %), (iii) milli-Q water, (iv) phosphate buffered saline, and (v) a GalN-NPmoc dispersion (sol) prepared using 100 mM HEPES–NaOH (pH 7.4) containing DMSO (5.0 vol %). [GlcN- or GalN-NPmoc] = 0.75 wt %. Please see Figure S6 for more details. (B) Frequency and strain sweep (0.20% strain for frequency sweep and 1.0  $\text{rad s}^{-1}$  for strain sweep) rheological properties of GlcN-NPmoc hydrogels {[GlcN-NPmoc] = 0.75 and 1.0 wt %, 100 mM HEPES–NaOH (pH 7.4) containing DMSO (5.0 vol %):  $G'$ , storage modulus;  $G''$ , loss modulus} at 25 °C.

the previous report on Fmoc hydrogels, in which both derivatives (GlcN- and GalN-Fmoc) demonstrated hydrogel formation ability.<sup>13a</sup> We presume that the axial OH group at the C4 position in the GalN group of GalN-NPmoc may hinder the formation of self-assembled network structures (nanofiber network, vide infra), which is required for hydrogel formation. As shown in Figure 1C, in a single crystal structure of *N*-acetyl- $\alpha$ -D-glucosamine ( $\alpha$ -D-GlcNAc, AGLUA10),<sup>18a</sup> one-dimensional columnar structure is stabilized by hydrogen bonding interaction between the neighboring C2-amide groups, from which an energy-minimized self-assembled structure of GlcN-NPmoc was obtained as the plausible model. In the model,  $\pi$ - $\pi$  stacking interaction of nitrophenyl groups and interactions in the one-dimensional columnar structure of  $\alpha$ -D-GlcNAc moiety can function cooperatively. In contrast, such a hydrogen bonding interaction between the neighboring C2-amide groups is absent in a single crystal structure of *N*-acetyl- $\alpha$ -D-galactosamine ( $\alpha$ -D-GalNAc, AGALAM10)<sup>18b</sup> but C4-OH group is incorporated into the hydrogen bonding network with C3-OH group from the other one-dimensional columnar structure. This difference may have an influence on the hydrogel (nanofiber) formation ability of GlcN-NPmoc and GalN-NPmoc. We speculate that the strong tendency of the Fmoc group in GalN-Fmoc to induce the one-dimensional self-assembly<sup>19</sup> compared with the less hydrophobic and smaller aromatic NPmoc group may overcome the hampering effect of the axial OH group at C4 position in the pyranose ring to form nanofiber.

To investigate the morphology of the self-assembled structures, transmission electron microscopy (TEM) observations were performed. As shown in Figure 3Ai, GlcN-NPmoc

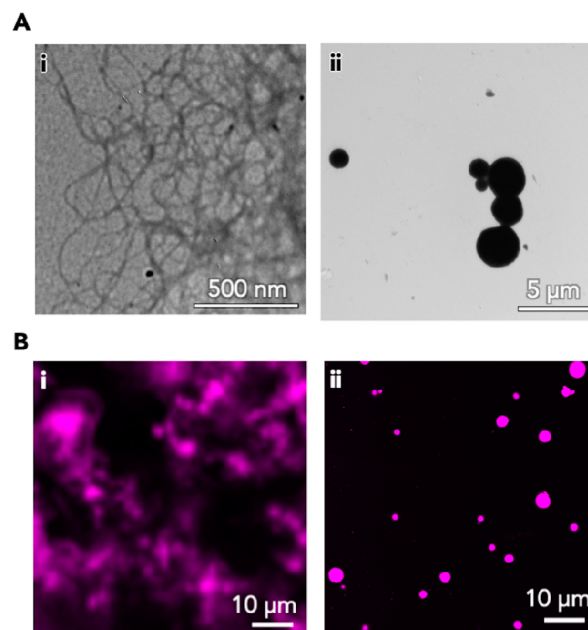


**Figure 3.** Representative (A) TEM and (B) CLSM images of (i) the GlcN-NPmoc hydrogel and (ii) the GalN-NPmoc dispersion (sol). Details on the CLSM observation protocols are described in the Experimental Section.

produced nanofiber networks, which is characteristic of supramolecular hydrogels.<sup>1,7,10</sup> Meanwhile, GalN-NPmoc formed non-networked spherical structures, as seen in Figure 3Aii. This obvious morphological difference is consistent with their distinct hydrogel formation ability. To probe the morphology without drying the samples, we subjected the GlcN-NPmoc hydrogel and GalN-NPmoc sol to in situ confocal laser scanning microscopy (CLSM) observation. Upon the addition of Nile Red as a typical hydrophobic fluorescent probe,<sup>10k</sup> an aggregated fibrous network and spherical structures were visualized for GlcN- and GalN-NPmoc, respectively, as shown in Figure 3B. The smaller average size of the spherical structures of GalN-NPmoc ( $1.8 \pm 0.8 \mu\text{m}$ ) in the TEM images compared with that in the CLSM images ( $2.5 \pm 1.4 \mu\text{m}$ ) could be ascribed to the influence of drying the sample for the TEM observations. Interestingly, we found that similar structures were observed with CLSM when using a fluorescent probe bearing a hydrazide group (4-hydrazino-7-nitro-2,1,3-benzoxadiazole, NBD-H<sup>20</sup>), as presented in Figure 4, which can be attributed to the formation of a hydrazone bond between NBD-H and the reducing end of the sugar moiety in GlcN- and GalN-NPmoc. This reactivity has been scarcely explored for this class of sugar-based self-assembling molecules because most of them lack a reducing end in the sugar moiety, which enabled post-self-assembly functionalization of the present supramolecular architecture via dynamic covalent chemistry.<sup>21</sup>

To gain further insight into the present system and elucidate the self-assembly mode of GlcN-NPmoc in the hydrogel state, we conducted spectroscopic studies. As shown in Figures 5 and S7, the circular dichroism (CD) spectrum of the GlcN-NPmoc hydrogel displayed a bisignate CD signal with a negative peak

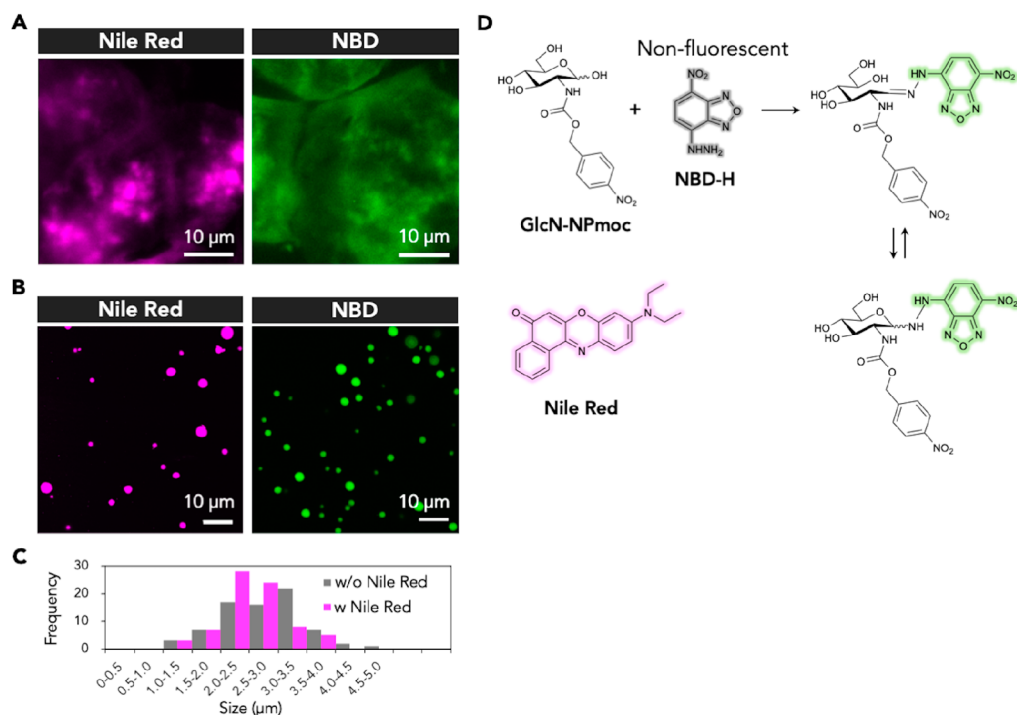


**Figure 4.** Representative CLSM images of (A) GlcN-NPmoc hydrogel and (B) GalN-NPmoc dispersion (sol) stained with Nile Red (left, magenta) or NBD-H (right, green). (C) Histogram analysis of the size of GalN-NPmoc microspheres (evaluated from DIC images) with or without Nile Red staining. (D) Chemical structures of Nile Red and NBD-H and reaction scheme between GlcN-NPmoc (self-assembled or not) and NBD-H, which should give rise to fluorescent molecules through hydrazone bond formation.<sup>20</sup> Conditions: [GlcN-NPmoc or GalN-NPmoc] = 0.91 wt % (26 mM), for Nile Red staining: [Nile Red] = 55 μM in an aqueous mixture (a:b = 10:1 (v/v)) of (a) 50 mM MES-NaOH (pH 5.5) containing DMSO (5.0 vol %) and (b) 50 mM MES-NaOH (pH 5.5) containing DMSO (2.0 vol %), or NBD staining: [NBD-H] = 4.5 mM in an aqueous mixture (a:b = 10:1 (v/v)) of (a) 50 mM MES-NaOH (pH 5.5) containing DMSO (5.0 vol %) and (b) DMSO, rt.

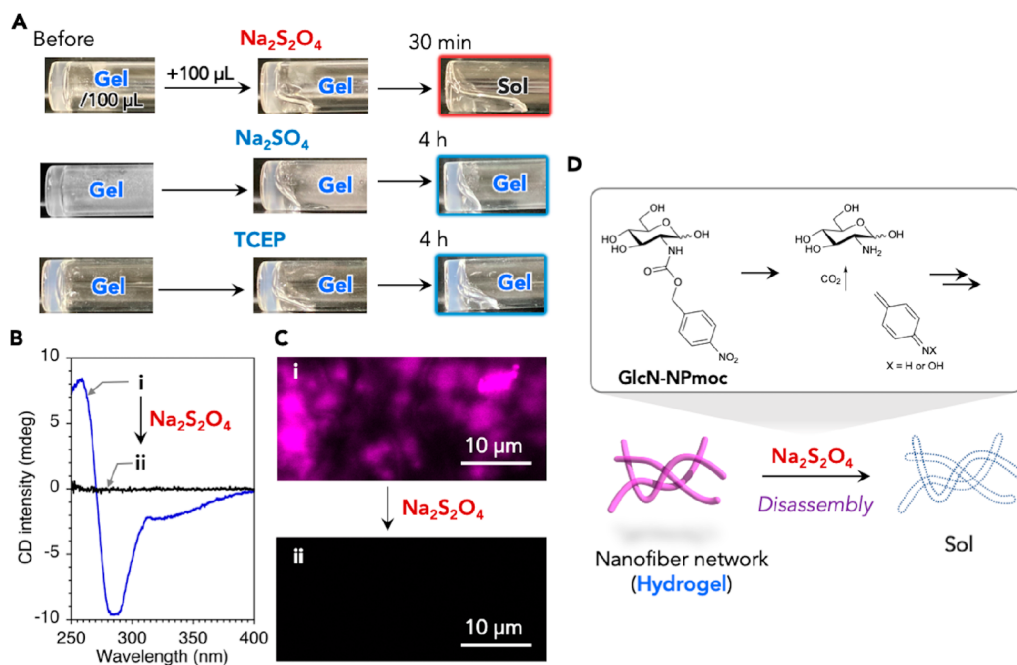


**Figure 5.** (A) Photographs of GlcN-NPmoc hydrogels [1.0 wt % (28 mM), 100 mM HEPES–NaOH (pH 7.4), 100 μL] before and after the addition of aqueous solutions (100 μL) containing Na<sub>2</sub>S<sub>2</sub>O<sub>4</sub> or Na<sub>2</sub>SO<sub>4</sub> (20 equiv) or TCEP (1.0 equiv) as external stimuli at room temperature. (B) CD spectra and (C) CLSM images of the GlcN-NPmoc hydrogel [1.0 wt % (28 mM), 100 mM HEPES–NaOH (pH 7.4)] (i) before and (ii) after the addition of Na<sub>2</sub>S<sub>2</sub>O<sub>4</sub> (20 equiv) at room temperature. (D) Scheme showing the Na<sub>2</sub>S<sub>2</sub>O<sub>4</sub>-responsive gel-to-sol transition of the GlcN-NPmoc hydrogel and the corresponding chemical transformation of the GlcN-NPmoc molecule.

at 286 nm and a positive peak at 258 nm, which is assignable to an exciton coupling between individual  $\pi$ – $\pi^*$  transitions of the

nitrophenyl group centered at 276 nm ( $\lambda_{\max}$ ). This putatively assigned negative exciton CD couplet suggests negative

chirality for the asymmetric arrangement (preferably left-handed) of the nitrophenyl moiety in the self-assembled state. Indeed, this CD signal disappeared at the concentration lower than 0.1 wt % (Figure S7A). The FTIR spectrum of the GlcN-NPmoc hydrogel (prepared with D<sub>2</sub>O at 3.0 wt % concentration, almost the same CD signals was observed even in D<sub>2</sub>O (Figure S7B)) showed a distinct peak assignable to carbonyl stretching of the carbamate bond of the NPmoc group at 1664 cm<sup>-1</sup> (Figure S8), which is shifted to a slightly lower energy compared with that of an NPmoc-containing water-soluble compound (see the Supporting Information for details) appearing at 1685 cm<sup>-1</sup>. This suggests the importance of hydrogen bonding interactions in the self-assembled structures of GlcN-NPmoc. Collectively, these results are consistent with the plausible model of self-assembled GlcN-NPmoc as fibrous nanostructures in the hydrogel state proposed above (Figure 1C).

With this new nitro group-containing supramolecular hydrogelator based on an amino sugar (GlcN-NPmoc hydrogel) in hand, we next investigated its reduction-responsive property. By carefully adding an aqueous solution (100 μL) containing Na<sub>2</sub>S<sub>2</sub>O<sub>4</sub> as a chemical reductant (20 equiv. against GlcN-NPmoc) onto the GlcN-NPmoc hydrogel (1.0 wt %, 28 mM, 100 μL), macroscopic gel-to-sol transition (gel degradation) was observed within 30 min at room temperature, as shown in Figure 5A. In contrast, upon the addition of the same amount of nonreductant Na<sub>2</sub>SO<sub>4</sub>, no gel degradation was observed, suggesting that the influence of increased salt concentration on the Na<sub>2</sub>S<sub>2</sub>O<sub>4</sub>-induced gel degradation was not significant. Moreover, the addition of tris(2-carboxyethyl)phosphine hydrochloride (TCEP, 1.0 equiv. against GlcN-NPmoc) in an amount that would be sufficient to induce the cleavage of disulfide bonds according to a recent report<sup>7c</sup> did not induce gel degradation. Similarly, no gel degradation was observed by the addition of reduced glutathione (1.0 eq. against GlcN-NPmoc, Figure S9). Collectively, these results indicate that the Na<sub>2</sub>S<sub>2</sub>O<sub>4</sub>-induced gel degradation correlates with the chemical reduction of the nitro group, whose selectivity is consistent with previous reports.<sup>7g</sup> The CD spectrum recorded 30 min after the addition of Na<sub>2</sub>S<sub>2</sub>O<sub>4</sub> showed that the original bisignate CD signal (Figure 5B) virtually disappeared, which was associated with the disappearance of the absorption peak at ~276 nm assignable to the nitrophenyl group (Figure S7C). In addition, CLSM observations revealed the evanescence of the aggregated fibrous network within 30 min after the addition of Na<sub>2</sub>S<sub>2</sub>O<sub>4</sub> (Figure 5C). To further evaluate the gel degradation or retention in response to chemical stimuli described above, we monitored the Brownian motion of hydrophilic fluorescent silica nanobeads embedded in the gel samples (500 nm in diameter, the size of which is expected to be smaller than the mesh size of typical supramolecular hydrogels<sup>6a</sup>) by CLSM. As shown in Figure S10, suppressed Brownian motion of the nanobeads was observed in the initial gel state, which indicates that the nanobeads were entrapped by the nanofiber networks. By contrast, almost free Brownian motion of the nanobeads was observed within 30 min after the addition of Na<sub>2</sub>S<sub>2</sub>O<sub>4</sub>, which should be correlated with the macroscopic gel degradation. On the other hand, suppressed Brownian motion of the nanobeads was still observed even 30 min after the addition of Na<sub>2</sub>SO<sub>4</sub> and TCEP, suggesting the persistence of the nanofiber networks. Collectively, these CLSM observation results on the Brownian motion of

nanobeads are well consistent with the macroscopic gel degradation or retention behaviors in response to the different chemical stimuli.

The reduction response, i.e., the reduction of the nitro group, of GlcN-NPmoc induced by Na<sub>2</sub>S<sub>2</sub>O<sub>4</sub> was further investigated by <sup>1</sup>H NMR spectroscopy (Figure S11), which was conducted after dissolution of the samples in DMSO-*d*<sub>6</sub> (for a gel prepared with D<sub>2</sub>O and sol after Na<sub>2</sub>S<sub>2</sub>O<sub>4</sub>-induced gel degradation, a similar responsiveness was validated). We found that the signals attributable to the NPmoc group (nitrophenyl and benzyl protons) almost completely disappeared after the Na<sub>2</sub>S<sub>2</sub>O<sub>4</sub>-induced gel degradation, whereas new multiple peaks assignable to (hydroxyl)aminophenyl groups (~6.5–7.3 ppm) appeared. The presence of other new multiple peaks in the region ~4.7–4.9 ppm, which could be assigned to benzylic protons, suggests that several compounds were generated, most probably through the reaction between quinoneimine methide (released from GlcN-NPmoc via reduction-triggered 1,6-elimination) and nucleophiles including a water molecule and the amino group of the generated glucosamine.<sup>7g</sup> Indeed, similar spectral change was observed for the NPmoc-containing water-soluble compound used in IR study (vide supra) upon the addition of Na<sub>2</sub>S<sub>2</sub>O<sub>4</sub> under the same conditions (Figure S12). In contrast, almost no spectral change was observed upon the addition of TCEP, which induced no gel degradation. Taken together, these results support our view that the reductant Na<sub>2</sub>S<sub>2</sub>O<sub>4</sub> triggered the macroscopic gel-to-sol transition of the GlcN-NPmoc hydrogel through the reduction of the nitro group and the subsequent removal of the NPmoc group from GlcN-NPmoc via 1,6-elimination,<sup>7g,15</sup> which eventually induced the disassembly of the supramolecular architectures (gel degradation) due to the conversion of the supramolecular hydrogelator GlcN-NPmoc into nonself-assembling molecules. All the components of this complex mixture are not fully assigned yet (Figure 5D).

## CONCLUSION

In summary, we developed a glucosamine-based supramolecular hydrogelator capable of spontaneously forming supramolecular nanofibers via aqueous self-assembly, producing a reduction-responsive supramolecular hydrogel. This compact but modular molecularly designed hydrogelator, which can be synthesized in only one step using two commercially available compounds as the minimal starting materials, is one of the simplest low-molecular-weight supramolecular hydrogelators affording reduction-responsive supramolecular hydrogels. The robustness of the present modular molecular design<sup>22</sup> and its synthetic simplicity could enable further development of various reduction-responsive aqueous nano- and soft-materials with improved properties and functions. For example, the properties and functions of supramolecular microspheres of galactosamine-based molecules should be further explored; however, this is beyond the scope of this paper focusing on supramolecular hydrogels. Furthermore, bioapplications of stimuli-responsive supramolecular hydrogels, such as in regenerative medicine and cosmetics, may become a target of research in the near future.

## EXPERIMENTAL SECTION

Detailed experimental procedures for the synthesis of GlcN-NPmoc and GalN-NPmoc can be found in the Supporting Information.

### Conventional Hydrogelation Ability Test

The gelation ability was evaluated by an inverted tube test. Typically, a DMSO stock solution of GlcN-NPmoc (200 mg/mL, 10  $\mu$ L) was mixed with 100 mM HEPES-NaOH buffer (pH 7.4, 190  $\mu$ L) to obtain an aqueous dispersion (1.0 wt %, 28 mM) in a glass vial. The resultant solution was applied with sonication and heated by a heat gun. When a transparent aqueous solution was obtained, the solution was cooled down at room temperature for a designated time and the hydrogel formation was evaluated by inverting the glass vial.

### CLSM Observation

A GlcN-NPmoc hydrogel or a GalN-NPmoc dispersion [1.0 wt %, 100 mM HEPES-NaOH (pH 7.4, 10  $\mu$ L) or 50 mM MES-NaOH (pH 5.5, 10  $\mu$ L) containing DMSO (5.0 vol %)] obtained according to the procedure described above was mixed with an aqueous DMSO (2.0 vol %) solution of Nile Red (600  $\mu$ M, 1.0  $\mu$ L) or a DMSO solution of NBD-H (50 mM, 1.0  $\mu$ L) and spotted on a glass coverslip (diameter: 25 mm, thickness: 0.13–0.17 mm, Fisher Scientific) placed in Attofluor cell chamber (Thermo Fisher Scientific) with water drops (ca. 50  $\mu$ L) around the sample drop to avoid dryness. Confocal laser scanning fluorescence microscopy (CLSM) observations were performed with an FV1000-D microscope (IX81, Olympus) equipped with a LED laser (559 nm) for Nile Red, an Ar laser (488 nm) for NBD, and a gallium arsenide phosphide (GaAsP) detector. A 60 $\times$  (numerical aperture (NA) = 1.49) oil objective was employed to obtain images (typically, 1024  $\times$  1024 pixel). The images were obtained and analyzed by the acquisition software FV10-ASW4.2 equipped with the microscope.

### Reduction-Responsive Gel-to-Sol Transition of GlcN-NPmoc Hydrogel

Typically, to a GlcN-NPmoc hydrogel [1.0 wt %, 100 mM HEPES-NaOH (pH 7.4, 200  $\mu$ L) containing DMSO (5.0 vol %)] was added an aqueous solution of Na<sub>2</sub>S<sub>2</sub>O<sub>4</sub> (1.1 M, 100  $\mu$ L, 20 equiv.) and the resultant sample was incubated at room temperature for a designated time. The stimuli-responsive gel-to-sol transition was carefully evaluated by an inverted tube test. As a negative control experiment, an aqueous solution of Na<sub>2</sub>SO<sub>4</sub> (1.1 M, 100  $\mu$ L, 20 equiv.) or TCEP (56 mM, 100  $\mu$ L, 1.0 equiv.) was added instead of the aqueous solution of Na<sub>2</sub>S<sub>2</sub>O<sub>4</sub>.

### ASSOCIATED CONTENT

#### Supporting Information

The Supporting Information is available free of charge at <https://pubs.acs.org/doi/10.1021/jacsau.1c00270>.

Materials and experimental procedures, synthetic procedures and characterizations of new compounds, characterizations of supramolecular hydrogels (gelation ability, CD spectra, FTIR spectra, stimuli-responsiveness, <sup>1</sup>H NMR spectra) (Figures S1–S12 and Scheme S1) (PDF)

### AUTHOR INFORMATION

#### Corresponding Author

Masato Ikeda – United Graduate School of Drug Discovery and Medical Information Sciences, Gifu University, Gifu 501-1193, Japan; Department of Chemistry and Biomolecular Science, Faculty of Engineering and Institute for Glyco-core Research (iGCORE), Gifu University, Gifu 501-1193, Japan; Center for Highly Advanced Integration of Nano and Life Sciences, Gifu University (G-CHAIN), Gifu 501-1193, Japan; Institute of Nano-Life-Systems, Institutes of Innovation for Future Society, Nagoya University, Furo-cho, Chikusa-ku, Nagoya 464-8603, Japan; [orcid.org/0000-0003-4097-8292](https://orcid.org/0000-0003-4097-8292); Email: [m\\_ikeda@gifu-u.ac.jp](mailto:m_ikeda@gifu-u.ac.jp)

### Author

Sayuri L. Higashi – United Graduate School of Drug Discovery and Medical Information Sciences, Gifu University, Gifu 501-1193, Japan

Complete contact information is available at: <https://pubs.acs.org/10.1021/jacsau.1c00270>

### Author Contributions

M.I. conceived the project. S.L.H. and M.I. designed and conducted the experiments. The manuscript was written through contributions of all authors. All authors have given approval to the final version of the manuscript.

### Notes

The authors declare no competing financial interest.

### ACKNOWLEDGMENTS

This work was supported in part by financial support from KOSÉ Cosmetology Research Foundation. S.L.H. thanks JSPS Research Fellowship for Young Scientists. The authors thank Mr. Koichiro M. Hirose and Prof. Kenichi G.N. Suzuki for their kind permission to use the CLSM facility and support. The authors acknowledge Life Science Research Center and Research Equipment Sharing Promotion Center, Gifu University for the maintenance of the instruments and their kind support. The authors thank Enago ([www.enago.jp](http://www.enago.jp)) for the English language review.

### REFERENCES

- (a) Estroff, L. A.; Hamilton, A. D. Water Gelation by Small Organic Molecules. *Chem. Rev.* **2004**, *104*, 1201–1218. (b) de Loos, M.; Feringa, B. L.; van Esch, J. H. Design and Application of Self-Assembled Low Molecular Weight Hydrogels. *Eur. J. Org. Chem.* **2005**, *2005*, 3615–3631. (c) Du, X.; Zhou, J.; Shi, J.; Xu, B. Supramolecular Hydrogelators and Hydrogels: From Soft Matter to Molecular Biomaterials. *Chem. Rev.* **2015**, *115*, 13165–13307. (d) Draper, E. R.; Adams, D. J. Low-Molecular-Weight Gels: The State of the Art. *Chem.* **2017**, *3*, 390–410. (e) Shigemitsu, H.; Hamachi, I. Design Strategies of Stimuli-Responsive Supramolecular Hydrogels Relying on Structural Analyses and Cell-Mimicking Approaches. *Acc. Chem. Res.* **2017**, *50*, 740–750. (f) Gelain, F.; Luo, Z.; Zhang, S. Self-Assembling Peptide EAK16 and RADA16 Nanofiber Scaffold Hydrogel. *Chem. Rev.* **2020**, *120*, 13434–13460.
- (1) Li, Y.; Wang, F.; Cui, H. Peptide-based Supramolecular Hydrogels for Delivery of Biologics. *Bioengineering & Translational Medicine* **2016**, *1*, 306–322.
- (2) Ikeda, M.; Ochi, R.; Hamachi, I. Supramolecular Hydrogel-Based Protein and Chemosensor Array. *Lab Chip* **2010**, *10*, 3325–3334.
- (3) (a) Dou, X.-Q.; Feng, C.-L. Amino Acids and Peptide-Based Supramolecular Hydrogels for Three-Dimensional Cell Culture. *Adv. Mater.* **2017**, *29*, 1604062. (b) He, H.; Xu, B. Instructed-Assembly (iA): A Molecular Process for Controlling Cell Fate. *Bull. Chem. Soc. Jpn.* **2018**, *91*, 900–906. (c) Maruyama, T.; Restu, W. K. Intracellular Self-Assembly of Supramolecular Gelators to Selectively Kill Cells of Interest. *Polym. J.* **2020**, *52*, 883–889.
- (4) Raeburn, J.; Zamith Cardoso, A.; Adams, D. J. The Importance of The Self-Assembly Process to Control Mechanical Properties of Low Molecular Weight Hydrogels. *Chem. Soc. Rev.* **2013**, *42*, 5143–5156.
- (5) (a) Matsumoto, S.; Yamaguchi, S.; Ueno, S.; Komatsu, H.; Ikeda, M.; Ishizuka, K.; Iko, Y.; Tabata, K.; Aoki, H.; Ito, S.; Noji, H.; Hamachi, I. Photo Gel-Sol/Sol-Gel Transition and Its Patterning of a Supramolecular Hydrogel as Stimuli-Responsive Biomaterials. *Chem. - Eur. J.* **2008**, *14*, 3977–3986. (b) Larik, F. A.; Fillbrook, L. L.; Nurttala, S. S.; Martin, A. D.; Kuchel, R. P.; Al Taieff, K.; Bhadbhade, M.; Beves, J. E.; Thordarson, P. Ultra-Low Molecular Weight

Photoswitchable Hydrogelators. *Angew. Chem., Int. Ed.* **2021**, *60*, 6764–6770.

(7) (a) Weiss, R. G.; Terech, P. *Molecular Gels: Materials with Self-Assembled Fibrillar Networks*; Springer, 2006; Chapters 17 and 18. (b) Menger, F. M.; Caran, K. L. Anatomy of a Gel. Amino Acid Derivatives That Rigidify Water at Submillimolar Concentrations. *J. Am. Chem. Soc.* **2000**, *122*, 11679–11691. (c) Wojciechowski, J. P.; Martin, A. D.; Thordarson, P. Kinetically Controlled Lifetimes in Redox-Responsive Transient Supramolecular Hydrogels. *J. Am. Chem. Soc.* **2018**, *140*, 2869–2874. (d) Li, X.; Li, J.; Gao, Y.; Kuang, Y.; Shi, J.; Xu, B. Molecular Nanofibers of Olsalazine Form Supramolecular Hydrogels for Reductive Release of an Anti-inflammatory Agent. *J. Am. Chem. Soc.* **2010**, *132*, 17707–17709. (e) Sun, Z.; Li, Z.; He, Y.; Shen, R.; Deng, L.; Yang, M.; Liang, Y.; Zhang, Y. Ferrocenyl Phenylalanine: A New Strategy Toward Supramolecular Hydrogels with Multistimuli Responsive Properties. *J. Am. Chem. Soc.* **2013**, *135*, 13379–13386. (f) Miao, X.; Cao, W.; Zheng, W.; Wang, J.; Zhang, X.; Gao, J.; Yang, C.; Kong, D.; Xu, H.; Wang, L.; Yang, Z. Switchable Catalytic Activity: Selenium-Containing Peptides with Redox-Controllable Self-Assembly Properties. *Angew. Chem., Int. Ed.* **2013**, *52*, 7781–7785. (g) Ikeda, M.; Tanida, T.; Yoshii, T.; Hamachi, I. Rational Molecular Design of Stimulus-Responsive Supramolecular Hydrogels Based on Dipeptides. *Adv. Mater.* **2011**, *23*, 2819–2822. (h) Ikeda, M.; Tanida, T.; Yoshii, T.; Kurotani, K.; Onogi, S.; Urayama, K.; Hamachi, I. Installing Logic-Gate Responses to a Variety of Biological Substances in Supramolecular Hydrogel–Enzyme Hybrids. *Nat. Chem.* **2014**, *6*, 511–518. (i) Shigemitsu, H.; Fujisaku, T.; Onogi, S.; Yoshii, T.; Ikeda, M.; Hamachi, I. Preparation of Supramolecular Hydrogel–Enzyme Hybrids Exhibiting Biomolecule-Responsive Gel Degradation. *Nat. Protoc.* **2016**, *11*, 1744–1756. (8) Wilson, W.; Hay, M. Targeting Hypoxia in Cancer Therapy. *Nat. Rev. Cancer* **2011**, *11*, 393–410.

(9) For recent reviews: (a) Gronwald, O.; Shinkai, S. Sugar-Integrated Gelators of Organic Solvents. *Chem. - Eur. J.* **2001**, *7*, 4328–4334. (b) Datta, S.; Bhattacharya, S. Multifarious Facets of Sugar-Derived Molecular Gels: Molecular Features, Mechanisms of Self-Assembly and Emerging Applications. *Chem. Soc. Rev.* **2015**, *44*, 5596–5637. (c) Delbianco, M.; Bharate, P.; Varela-Aramburu, S.; Seiberger, P. H. Carbohydrates in Supramolecular Chemistry. *Chem. Rev.* **2016**, *116*, 1693–1752.

(10) (a) Fuhrhop, J. H.; Schnieder, P.; Rosenberg, J.; Boekema, E. The Chiral Bilayer Effect Stabilizes Micellar Fibers. *J. Am. Chem. Soc.* **1987**, *109*, 3387–3390. (b) Jung, J. H.; Shinkai, S.; Shimizu, T. Spectral Characterization of Self-Assemblies of Aldopyranoside Amphiphilic Gelators: What is the Essential Structural Difference between Simple Amphiphiles and Bolaamphiphiles. *Chem. - Eur. J.* **2002**, *8*, 2684–2690. (c) Friggeri, A.; Gronwald, O.; van Bommel, K. J. C.; Shinkai, S.; Reinhoudt, D. N. Charge-Transfer Phenomena in Novel, Dual-Component, Sugar-Based Organogels. *J. Am. Chem. Soc.* **2002**, *124*, 10754–10758. (d) Kiyonaka, S.; Sugiyasu, K.; Shinkai, S.; Hamachi, I. First Thermally Responsive Supramolecular Polymer Based on Glycosylated Amino Acid. *J. Am. Chem. Soc.* **2002**, *124*, 10954–10955. (e) Roytman, R.; Adler-Abramovich, L.; Kumar, K. S. A.; Kuan, T.-C.; Lin, C.-C.; Gazit, E.; Brik, A. Exploring the Self-Assembly of Glycopeptides Using a Diphenylalanine Scaffold. *Org. Biomol. Chem.* **2011**, *9*, 5755–5761. (f) Clemente, M. J.; Fitremann, J.; Mauzac, M.; Serrano, J. L.; Oriol, L. Synthesis and Characterization of Maltose-Based Amphiphiles as Supramolecular Hydrogelators. *Langmuir* **2011**, *27*, 15236–15247. (g) Ikeda, M.; Ochi, R.; Kurita, Y.-s.; Pochan, D. J.; Hamachi, I. Heat-Induced Morphological Transformation of Supramolecular Nanostructures by Retro-Diels–Alder Reaction. *Chem. - Eur. J.* **2012**, *18*, 13091–13096. (h) Ochi, R.; Kurotani, K.; Ikeda, M.; Kiyonaka, S.; Hamachi, I. Supramolecular Hydrogels Based on Bola-Amphiphilic Glycolipids Showing Color Change in Response to Glycosidases. *Chem. Commun.* **2013**, *49*, 2115–2117. (i) Latxague, L.; Ramin, M. A.; Appavoo, A.; Berto, P.; Maisani, M.; Ehret, C.; Chassande, O.; Barthélémy, P. Control of Stem-Cell Behavior by Fine Tuning the Supramolecular Assemblies of Low-Molecular-Weight Gelators. *Angew. Chem., Int. Ed.* **2015**, *54*,

4517–4521. (j) Liu, J.; Sun, Z.; Yuan, Y.; Tian, X.; Liu, X.; Duan, G.; Yang, Y.; Yuan, L.; Lin, H.-C.; Li, X. Peptide Glycosylation Generates Supramolecular Assemblies from Glycopeptides as Biomimetic Scaffolds for Cell Adhesion and Proliferation. *ACS Appl. Mater. Interfaces* **2016**, *8*, 6917–6924. (k) Tsuzuki, T.; Kabumoto, M.; Arakawa, H.; Ikeda, M. The Effect of Carbohydrate Structures on the Hydrogelation Ability and Morphology of Self-Assembled Structures of Peptide–Carbohydrate Conjugates in Water. *Org. Biomol. Chem.* **2017**, *15*, 4595–4600. (l) Akama, S.; Maki, T.; Yamanaka, M. Enzymatic Hydrolysis-Induced Degradation of a Lactose-Coupled Supramolecular Hydrogel. *Chem. Commun.* **2018**, *54*, 8814–8817. (m) Restuccia, A.; Seroski, D. T.; Kelley, K. L.; O'Bryan, C. S.; Kurian, J. J.; Knox, K. R.; Farhadi, S. A.; Angelini, T. E.; Hudalla, G. A. Hierarchical Self-Assembly and Emergent Function of Densely Glycosylated Peptide Nanofibers. *Commun. Chem.* **2019**, *2*, 53. (n) Biswakarma, D.; Dey, N.; Bhattacharya, S. A Thermo-Responsive Supramolecular Hydrogel That Senses Cholera Toxin via Color-Changing Response. *Chem. Commun.* **2020**, *56*, 7789–7792. (o) He, C.; Wu, S.; Liu, D.; Chi, C.; Zhang, W.; Ma, M.; Lai, L.; Dong, S. Glycopeptide Self-Assembly Modulated by Glycan Stereochemistry through Glycan–Aromatic Interactions. *J. Am. Chem. Soc.* **2020**, *142*, 17015–17023.

(11) Gama, C. I.; Hsieh-Wilson, L. C. Chemical Approaches to Deciphering the Glycosaminoglycan Code. *Curr. Opin. Chem. Biol.* **2005**, *9*, 609–619.

(12) (a) Yang, Z.; Liang, G.; Ma, M.; Abbah, A. S.; Lu, W. W.; Xu, B. D-Glucosamine-based Supramolecular Hydrogels to Improve Wound Healing. *Chem. Commun.* **2007**, 843–845. (b) Wang, G.; Cheuk, S.; Yang, H.; Goyal, N.; Reddy, P. V. N.; Hopkinson, B. Synthesis and Characterization of Monosaccharide-Derived Carbamates as Low-Molecular-Weight Gelators. *Langmuir* **2009**, *25*, 8696–8705.

(13) (a) Birchall, L. S.; Roy, S.; Jayawarna, V.; Hughes, M.; Irvine, E.; Okorogheye, G. T.; Saudi, N.; De Santis, E.; Tuttle, T.; Edwards, A. A.; Ulijn, R. V. Exploiting CH– $\pi$  Interactions in Supramolecular Hydrogels of Aromatic Carbohydrate Amphiphiles. *Chem. Sci.* **2011**, *2*, 1349–1355. (b) Pires, R. A.; Abul-Haija, Y. M.; Costa, D. S.; Novoa-Carballal, R.; Reis, R. L.; Ulijn, R. V.; Pashkuleva, I. Controlling Cancer Cell Fate Using Localized Biocatalytic Self-Assembly of an Aromatic Carbohydrate Amphiphile. *J. Am. Chem. Soc.* **2015**, *137*, 576–579.

(14) Very recently, Singh et al.<sup>14a</sup> reported that the addition of aqueous Na<sub>2</sub>S<sub>2</sub>O<sub>4</sub> to a hydrogel constructed from a monosaccharide-based supramolecular hydrogelator bearing an aldehyde group ( $M_w = 310.30$  g/mol)<sup>14b</sup> induced macroscopic gel-to-sol transition.<sup>14a</sup> It was therein demonstrated that the aldehyde is converted into a hydrophilic  $\alpha$ -hydroxy sulfonate through reversible nucleophilic addition of a bisulfite anion (HSO<sub>3</sub><sup>−</sup>), which is spontaneously generated by fragmentations of S<sub>2</sub>O<sub>4</sub><sup>2−</sup> in an aqueous solution, to the aldehyde.<sup>14a,c,d</sup> In fact, there is a discrepancy between ref 14a ( $\alpha$ -hydroxy sulfonate produced by reaction between aldehyde and HSO<sub>3</sub><sup>−</sup>) and ref 14d ( $\alpha$ -hydroxy sulfinate produced by the reaction between aldehyde and HSO<sub>2</sub><sup>−</sup>) for the intermediate of the complete reduction of aldehyde to alcohol by Na<sub>2</sub>S<sub>2</sub>O<sub>4</sub>. Nevertheless, to the best of our knowledge, this may be the lowest molecular weight hydrogelator<sup>14a,b</sup> exhibiting reductant responsiveness among the previously reported examples (Figure S1). (a) Singh, N.; Lainer, B.; Formon, G. J. M.; De Piccoli, S.; Hermans, T. M. Re-programming Hydrogel Properties Using a Fuel-Driven Reaction Cycle. *J. Am. Chem. Soc.* **2020**, *142*, 4083–4087. (b) Chen, Q.; Lv, Y.; Zhang, D.; Zhang, G.; Liu, C.; Zhu, D. Cysteine and pH-Responsive Hydrogel Based on a Saccharide Derivative with an Aldehyde Group. *Langmuir* **2010**, *26*, 3165–3168. (c) Kjell, D. P.; Slattery, B. J.; Semo, M. J. A Novel, Nonaqueous Method for Regeneration of Aldehydes from Bisulfite Adducts. *J. Org. Chem.* **1999**, *64*, 5722–5724. (d) de Vries, J. G.; Kellogg, R. M. Reduction of Aldehydes and Ketones by Sodium Dithionite. *J. Org. Chem.* **1980**, *45*, 4126–4129.

(15) Qian, X.; Hindsgaul, O. Use of the *p*-Nitrobenzyloxycarbonyl Group as an Orthogonal Amine Protecting Group in the Synthesis of

$\beta$ -GlcNAc Terminating Glycosides. *Chem. Commun.* **1997**, 1059–1060.

(16) Yan, C.; Pochan, D. J. Rheological Properties of Peptide-Based Hydrogels for Biomedical and Other Applications. *Chem. Soc. Rev.* **2010**, *39*, 3528–3540.

(17) (a) Sathaye, S.; Mbi, A.; Sonmez, C.; Chen, Y.; Blair, D. L.; Schneider, J. P.; Pochan, D. J. Rheology of Peptide- and Protein-Based Physical Hydrogels: Are Everyday Measurements Just Scratching the Surface? *Wiley Interdiscip. Rev.: Nanomed. Nanobiotechnol.* **2015**, *7*, 34–68. (b) Draper, E. R.; Mears, L. L. E.; Castilla, A. M.; King, S. M.; McDonald, T. O.; Akhtar, R.; Adams, D. J. Using the Hydrolysis of Anhydrides to Control Gel Properties and Homogeneity in pH-Triggered Gelation. *RSC Adv.* **2015**, *5*, 95369–95378. (c) Castilla, A. M.; Wallace, M.; Mears, L. L. E.; Draper, E. R.; Douth, J.; Rogers, S.; Adams, D. J. On the Syneresis of an OPV Functionalised Dipeptide Hydrogel. *Soft Matter* **2016**, *12*, 7848–7854.

(18) (a) Mo, F.; Jensen, L. H. A Refined Model for *N*-Acetyl- $\alpha$ -D-glucosamine. *Acta Crystallogr., Sect. B: Struct. Crystallogr. Cryst. Chem.* **1975**, *B31*, 2867–2873. (b) Neuman, A.; Gillier-Pandraud, H.; Longchambon, F.; Rabinovich, D. Structure Cristalline de la *N*-Acetyl- $\alpha$ -D-galactosamine. *Acta Crystallogr., Sect. B: Struct. Crystallogr. Cryst. Chem.* **1975**, *31*, 474–477. (c) Groom, C. R.; Bruno, I. J.; Lightfoot, M. P.; Ward, S. C. The Cambridge Structural Database. *Acta Crystallogr., Sect. B: Struct. Sci., Cryst. Eng. Mater.* **2016**, *B72*, 171–179.

(19) Tao, K.; Levin, A.; Adler-Abramovich, L.; Gazit, E. Fmoc-modified Amino Acids and Short Peptides: Simple Bio-Inspired Building Blocks for the Fabrication of Functional Materials. *Chem. Soc. Rev.* **2016**, *45*, 3935–3953.

(20) Uzu, S.; Kanda, S.; Imai, K.; Nakashima, K.; Akiyama, S. Fluorogenic Reagents: 4-Aminosulphonyl-7-hydrazino-2,1,3-benzoxadiazole, 4-(*N,N*-Dimethylaminosulphonyl)-7-hydrazino-2,1,3-benzoxadiazole and 4-Hydrazino-7-nitro-2,1,3-benzoxadiazole Hydrazine for Aldehydes and Ketones. *Analyst* **1990**, *115*, 1477–1482.

(21) (a) Sreenivasachary, N.; Lehn, J.-M. Gelation-driven Component Selection in the Generation of Constitutional Dynamic Hydrogels Based on Guanine-Quartet Formation. *Proc. Natl. Acad. Sci. U. S. A.* **2005**, *102*, 5938–5943. (b) Corbett, P. T.; Leclaire, J.; Vial, L.; West, K. R.; Wietor, J.-L.; Sanders, J. K. M.; Otto, S. Dynamic Combinatorial Chemistry. *Chem. Rev.* **2006**, *106*, 3652–3711. (c) Reuther, J. F.; Dahlhauser, S. D.; Anslyn, E. V. Tunable Orthogonal Reversible Covalent (TORC) Bonds: Dynamic Chemical Control over Molecular Assembly. *Angew. Chem., Int. Ed.* **2019**, *58*, 74–85. (d) Kubota, R.; Nagao, K.; Tanaka, W.; Matsumura, R.; Aoyama, T.; Urayama, K.; Hamachi, I. Control of Seed Formation Allows Two Distinct Self-Sorting Patterns of Supramolecular Nanofibers. *Nat. Commun.* **2020**, *11*, 4100.

(22) Ikeda, M. Stimuli-responsive Supramolecular Systems Guided by Chemical Reactions. *Polym. J.* **2019**, *51*, 371–380.